Periodic DFT Calculations of the Stability of Al/Si Substitutions and Extraframework Zn^{2+} Cations in Mordenite and Reaction Pathway for the Dissociation of H_2 and CH_4

L. Benco,*,†,‡ T. Bucko,† J. Hafner,† and H. Toulhoat§

Institut für Materialphysik and Center for Computational Materials Science, Universität Wien, Sensengasse 8, A-1090 Wien, Austria, Institute of Inorganic Chemistry, Slovak Academy of Sciences, Dubravska cesta 9, SK-84536 Bratislava, Slovak Republic, and Institut Français du Pétrole, F-92852 Rueil-Malmaison Cedex, France

Received: June 8, 2005; In Final Form: September 2, 2005

The local stability of Al atoms replacing Si in the zeolite framework is compared for all inequivalent tetrahedral (T) sites in mordenite. For Al/Si substitutions in two T sites the stable location of the compensating extraframework Zn^{2+} cation forming a Lewis acid site is determined. In the most stable Zn-MOR structures Zn^{2+} is located in a small ring (5MR, 6MR) containing two Al/Si substitutions. In less stable structures the Al atoms are placed at larger distances from each other and Zn^{2+} interacts with only one Al site. The simulated adsorption of H_2 and CH_4 shows that adsorption strength decreases with increasing stability of the Zn^{2+} Lewis site. A higher adsorption strength is observed for Zn^{2+} deposited in the 5MR than for the 6MR. The reactivity of a series of stable Zn^{2+} Lewis sites is tested via the dissociative adsorption of H_2 and CH_4. The heterolytic dissociation of the adsorbed molecule on the extraframework Zn^{2+} cation produces a proton and an anion. The anion binds to Zn^{2+} and proton goes to the zeolite framework, restoring a Brønsted acid site. Because bonding of the anion to Zn^{2+} is almost energetically equivalent for Zn^{2+} in any of the extraframework positions the dissociation is governed by stabilizing bonding of the proton to the framework. Those structures which can exothermically accommodate the proton represent reaction pathways. Due to the repulsion between the proton and Zn^{2+} the most favorable proton-accepting O sites are not those of the ring where Zn^{2+} is deposited, but O sites close to the ring. Large differences are observed for neighboring positions in *a*- and *b*-directions and those oriented along the *c*-vector. Finally, among the stable Zn^{2+} Lewis sites not all represent reaction pathways for dehydrogenation. For all of them the dissociation of H_2 is an exothermic process. In structures exhibiting the highest reactivity the Al/Si substitutions are placed at a large distance and the Zn^{2+} cation interacts with O-atoms next to Al in the T4 site of the 5MR. This Lewis site is strong enough to break the C−H bond in the CH_4 molecule.

1. Introduction

An extraframework Zn^{2+} cation in an ion-exchange position of a zeolite represents a Lewis site with high adsorption strength and reactivity. Such centers are active catalysts for dehydrogenation[1] and aromatization of light paraffins,[2−4] hydroamination,[5] and hydration of acetylene.[6] Many experimental studies have been focused on the determination of the location of the Zn^{2+} cation and on the characterization of its catalytically active forms.[7−12] In situ X-ray absorption studies suggest that Zn species reside as monomeric cations at cation-exchange sites.[8] With increased zinc loading additional extraframework cation sites are created and occupied with $(Zn-O-Zn)^{2+}$ species.[10] Such species are preferentially located in six-membered rings (6MR) bridging two Al/Si tetrahedral (T) sites. Monomeric Zn^{2+} cations are located in bridging positions between two AlO_4 tetrahedra. In low-Al zeolites (Si/Al = 25−40), however, the quantitative substitution of acid protons by Zn^{2+} cations indicates that Zn^{2+} cations can be located on isolated AlO_4 tetrahedra.[13]

The interesting properties of Zn-exchanged zeolites have attracted considerable attention of theoreticians. Zeolites are simulated by means of a fragment of the framework[14−23] or using realistic three-dimensional structures.[24−29] The former—the cluster approach—represents an attempt to apply techniques of molecular chemistry to bonding in the solid state. The latter—the periodic approach—utilizes the full periodicity of a crystalline solid. Most of the simulations of Zn-exchanged zeolites focus on finding stable extraframework Zn sites. Some studies assess the adsorption capacity of the Zn sites via the adsorption energies calculated for probe molecules, such as H_2O,[25] H_2,[19,21,22,26] and CH_4.[16,25,26] Only in a few papers is the reaction path for dissociative adsorption of molecules explored. Barbosa and van Santen applied the periodical approach to probe the reactivity of H_2 and CH_4 on $(Zn-O-Zn)^{2+}$ species in chabazite.[26] Properties of the monomeric Zn^{2+} cation deposited in small windows of the zeolite framework are simulated only by the cluster approach. Dissociative adsorption is reported for H_2,[19,21] CH_4,[16,22] ethane,[15,20] and butane.[29] For the adsorption of hydrocarbons an "alkyl path" for dissociation is observed, as suggested by Frash and van Santen,[15] producing a carbanion and not a carbenium ion. The dissociation occurs along the reaction pathway composed of both a Lewis and a Brønsted

* Address correspondence to this author. Phone: +43-1-4277-51407. Fax: +43-1-4277-9413. E-mail: lubomir.benco@univie.ac.at.
† Universität Wien.
‡ Slovak Academy of Sciences.
§ Institut Français du Pétrole.

10.1021/jp0530597 CCC: $30.25
Published on Web 10/04/2005

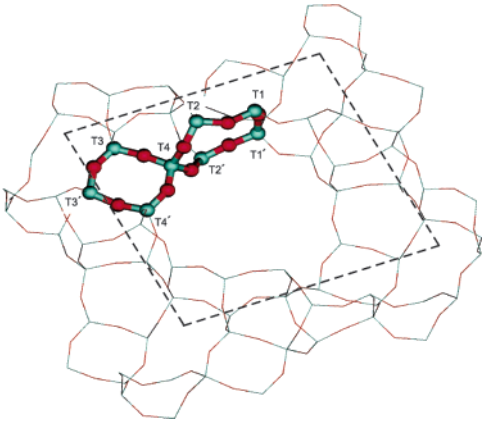

Figure 1. The structure of mordenite. Dotted lines indicate the *a* and *b* vectors spanning the basis plane of the monoclinic unit cell. Highlighted are four- and five-membered rings and the four inequivalent tetrahedral sites T1−T4.

acid site, taking advantage of the bifunctional character of the active form of the zeolite.

Although the use of small clusters provides reliable adsorption energies of molecules on zeolite active sites, considerable difficulties emerge in investigations of reactivity. In the conversion of the adsorbed molecule both the extraframework Lewis site and the framework Brønsted site play an active role. Accommodation of the dissociation products leads to considerable local deformation of the zeolite structure. A consideration of the real local structure and local deformability of the framework is therefore important for achieving reliable estimate of barriers along the reaction path. In the cluster approach the positions of several atoms are fixed to mimic the particular local configuration of the zeolite structure. Another reason for fixing atomic positions is the possible collapse of the structure during the relaxation of atomic positions. Both the constrained relaxation and the saturation of surface bonds with hydrogen atoms leads to considerable deformation of the potential energy surface. The cluster approach therefore appears to be much too simplistic for a simulation of the reactivity on Brønsted and Lewis sites of zeolites.

In the present work we use the real periodic structure of mordenite. We perform a complete analysis of the energetics of Al/Si substitutions in the zeolite framework and compare the stabilities of Zn-MOR structures with the extraframework Zn^{2+} cation anchored in all possible sites of both the main channel and the side channel of the mordenite structure. For the most stable Lewis sites we compare the adsorption energies of H_2 and CH_4. Finally, for the dissociative adsorption of H_2 and CH_4 on Zn^{2+} we explore the reaction pathways for intrazeolite conversions of the adsorbed molecules.

2. Structure and Computational Setup

The calculations are performed with the same monoclinic unit cell of mordenite, optimized for the purely siliceous structure[30] with the dimensions $a = b = 13.675$ Å, $c = 7.540$ Å, as recently used in our previous work.[31] Prior to Al/Si substitutions the cell contains 72 atoms: 24 tetrahedral (T) sites and 48 O sites. One Al/Si substitution in the T site produces a structure with a Si/Al ratio of 23. Two Al/Si substitutions used in calculations of Zn-MOR structures still keep the Si/Al ratio at the relatively high value of 11, typical for low-Al zeolites. A fraction of the structure, showing positions of four inequivalent T sites in the main and/or in the side channel, is displayed in Figure 1.

TABLE 1: Energetics of Single Al/Si Substitution; Energies (kJ/mol) of Two Equivalent Positions for T1 to T4 Sites Relative to the Most Stable T2 Site

	T1	T2	T3	T4
position 1	+4.2	0.0	+1.7	+7.4
position 2	+5.2	+0.6	+1.4	+7.5

The periodic density-functional theory (DFT) calculations are performed using the Vienna Ab initio Simulation Package (VASP).[32−35] The Kohn−Sham equations are solved by using the local exchange-correlation functional by Perdew and Zunger[36] corrected for nonlocality according to Perdew et al. (PW91).[37] Ultrasoft pseudopotentials[38,39] and a plane-wave basis set are used as implemented in the VASP package.[35] The calculations are performed with use of Blöchl's projector augmented wave technique[40,41] with a plane-wave cutoff energy of 400 eV. The Brillouin-zone sampling is restricted to the Γ point because such a restriction gives reliable results already for much smaller unit cells.[42]

3. Results

3.1. Framework Al/Si Substitutions. *3.1.1. Single Al/Si Substitution.* Table 1 shows the energetics for single Al/Si substitutions in each of the four inequivalent tetrahedral positions of the framework. The missing electron is compensated by an electron cloud uniformly smeared over the unit cell. The total energies thus do not depend on the position of the compensating cation and reflect the binding properties of the Al atom substituted in the respective tetrahedral site of the framework. The energy of the most stable location of the Al atom in the T2 site is taken as reference (cf. Table 1). For each T site the energies of two equivalent positions are presented. The total energies for substitutions in equivalent positions are not identical—the difference is largest for the T1 and T1′ sites (see Table 1). The origin of this discrepancy is in the slightly lower accuracy of the Hellmann−Feynmann forces calculated for a configuration with broken symmetry and the difficulties of a total-energy minimization in a multidimensional parameter space of low symmetry. Usually, Hellmann−Feynmann forces are symmetrized to minimize numerical errors. An isolated Al/Si substitution breaks the symmetry of the zeolite and without symmetrization slightly less accurate forces enter the relaxation routine. Hence the 1 kJ/mol discrepancy found for Al in the T1 and T1′ sites is a realistic upper bound for the uncertainty in the calculated energy differences.

Table 1 shows the differences in the total energies of single Al/Si substitutions in the four inequivalent T sites, calculated relative to the total energy of Al in the T2′ site. According to stabilities of the substituted structures the T sites are classified in two categories. The energies of the Al/Si substitutions in the T2 and T3 sites are similar (0−1.7 kJ/mol) and the corresponding structures are more stable than the structures created by substitution in the T1 or T4 site (4.2−7.5 kJ/mol). The lowest total energy is calculated for an Al/Si substitution in the T2 site located on the 5MR in the main channel of the mordenite structure. The substitution in the T3 site (1.4−1.7 kJ/mol) residing in the side channel appears only slightly less stable. A substitution in the T1 site of the main channel is energetically less favorable by 4.2−5.2 kJ/mol. The substitution in the T4 site, connecting the 5MR and the 4MR, carries a penalty of ∼7.5 kJ/mol.

The distribution of the Al atoms in the framework has been studied by Kato and co-workers for conventionally synthesized mordenite (CSM)[43] and for mordenite synthesized in the

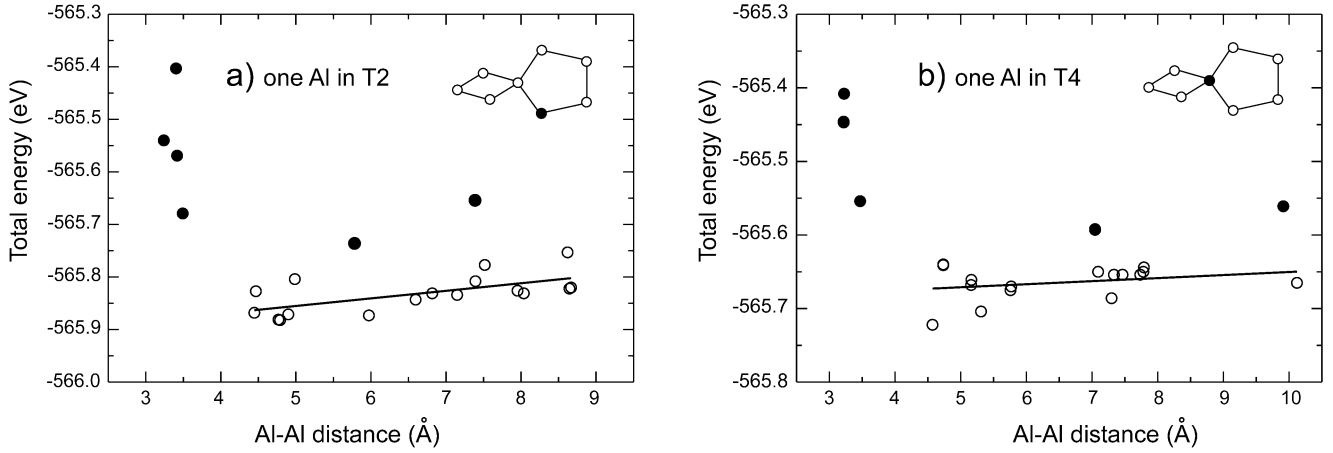

Figure 2. Energetics of the double Al/Si substitutions in mordenite as a function of the Al−Al distance. One Al is fixed in the more stable T2 site (a) or in the less stable T4 site (b) as highlighted in the inset. The second Al is placed in T sites extended throughout the cell. The full line is a least-squares fit excluding the nearest-neighbor positions and the energetically disadvantaged T4 sites (full circles).

presence of fluoride ion (FSM).[44] Their solid-state ^{29}Si MAS NMR measurements revealed that distribution of Al atoms depends on the structure directing agent. While in CSM Al atoms are located in all T sites, but in FSM only T1, T2, and T4 sites are occupied. With decreasing Al content Al atoms in T4 sites are first replaced by Si atoms, followed by Al atoms in T1 sites.[45] This observation agrees well with our calculated total energies. The dealumination of the framework occurs first for the least stable T4 site (+∼7.5 kJ/mol) and then for the T1 site (+∼5 kJ/mol).

3.1.2. Two Al/Si Substitutions. The energetics of the double Al/Si substitution is displayed in Figure 2. The calculations are performed without compensating cations with electron density of two electrons homogeneously smeared over the unit cell. Figure 2 shows the total energies calculated for two Al/Si substitution atoms placed in the framework at different distances. The position of one Al is fixed either in the less stable T4 site (Figure 2b) or in the more stable T2 site (Figure 2a). The second Al atom is placed in the T sites surrounding the site of the first Al/Si substitution.

The total energy is almost independent of the Al−Al distance with the exception of Al substitutions on nearest-neighbor T sites. For substitutions in these sites a penalty of 20−40 kJ/mol is observed. This is in line with the experimental Loewenstein rule excluding substitutions in the nearest-neighbor positions.[46] For locations of two Al atoms in the framework at a distance larger than ∼4 Å the total energy is almost constant. The scatter of calculated points reflects different stabilities of Al atoms in inequivalent T sites. The least stable structures, indicated with full circles, correspond to the second substitution in the least stable T4 site, in agreement with the energetics of single Al/Si substitutions (Table 1). The least-squares fits (full lines) suggest a slightly higher stability of Al/Si substitutions placed at short distances in second-neighbor positions. This finding is surprising since it predicts a high stability for two Al atoms located in the same small ring, like the 5MR and the 6MR. A good stability of structures with two Al atoms placed in the same small ring establishes a basis for a good stabilization of a divalent extraframework cation (cf. below.). The total energies for structures with one Al atom fixed in the less stable T4 site (Figure 2b) are by ∼15 kJ/mol higher than the total energies of structures with one Al atom in the T2 site (Figure 2a). This value corresponds to the energy difference between single Al/Si substitutions in the T2 and T4 sites multiplied by two (7.5 × 2 = 15 kJ/mol).

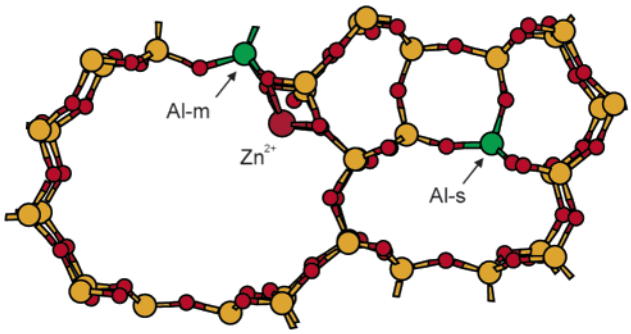

Figure 3. A Zn^{2+} cation stabilized by two AlO_4 tetrahedra located at a large distance. One Al is placed in the main channel (Al-m) and the second in the side channel (Al-s). The Zn^{2+} cation resides in the main channel.

3.2. Stability of Zn^{2+} in the Al/Si Substituted Structure. The stability of the extraframework Zn^{2+} cation deposited on the framework of a zeolite critically depends on the distance between the two Al sites carrying the compensating negative charges. Two basic situations can occur: a location of two Al atoms at short distance and a location at large distance. Al atoms placed at a short distance allow a direct contact of the Zn^{2+} cation with two compensating charges. In contrast, in a structure with Al/Si substitutions placed at a large distance the extraframework cation can interact only with one negatively charged framework site. The existence of metal-exchanged structures with the M^{2+} cation connected to only one Al/Si substitution is a matter of debate. The stabilization of the M^{2+} cation by AlO_4 tetrahedra separated by a large distance in the zeolite framework was recently shown by Kazansky et al.[12,47,48]

When the M^{2+} cation is connected to only one AlO_4 tetrahedron, the location of the cation depends on the character of the T site and on the local topology of the framework surrounding the T site. In mordenite the T1, T2, and T4 sites are situated in the main channel and the T3 site resides in the side channel.

3.2.1. Zn^{2+} Located Close to an Isolated Al/Si Substitution in the Main Channel. For the purpose of the investigation of the stability of a Zn^{2+} cation located near an isolated AlO_4 tetrahedron two Al atoms are placed at a large distance: one Al in the main channel and another in the side channel. An example of such a configuration is displayed in Figure 3.

For the Al/Si substitution in each of the inequivalent T1, T2, and T4 positions the accommodation of the Zn^{2+} cation in all

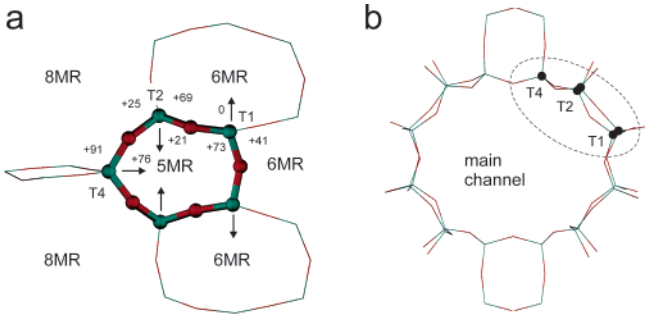

Figure 4. Relative stability of the extraframework Zn^{2+} cation interacting with one isolated Al/Si substitution in the main channel (a). For each T site the surrounding numbers stand for the total energies (in kJ/mol) of the Zn-exchanged zeolite with Al in the T site and the Zn^{2+} cation located in the ring (5MR, 6MR, 8MR) where the number is displayed. Arrows show the stable location of the Zn^{2+} cation if the Al atom resides in that particular T site. The location of T1, T2, and T4 sites in the main channel is sketched in part b. Energy differences are relative to a configuration with Al in a T1 site and Zn^{2+} in a 6MR (cf. Figure 5).

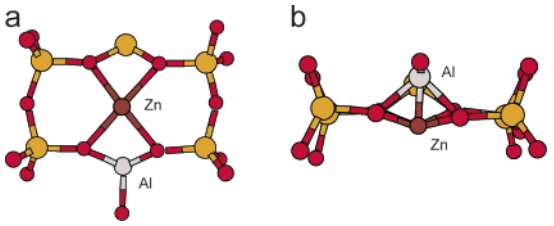

Figure 5. The most stable Zn-MOR structure for two Al sites placed at a large distance (cf. Figures 3 and 4). The Zn^{2+} cation is symmetrically accommodated in the 6MR. Side view (a) and top view along the main channel (b) showing that the extraframework cation resides almost exactly in the plane of the 6MR.

of the framework windows surrounding the particular T site is probed. For an Al/Si substitution in a T1 site, the Zn^{2+} cation can be placed either into the 5MR or in one of the two 6MR's sharing the T1 site. If the Al atom is located in a T2 site, possible locations of the Zn^{2+} cation are in the 5MR, the 6MR, and the larger 8MR circumscribing the side channel. For an Al atom in a T4 site, the Zn^{2+} cation may reside either within the 5MR or within one of the 8MR's sharing the T4 site. The relative stabilities are displayed in Figure 4. For each T site the energetically most favorable location of the Zn^{2+} cation is indicated by an arrow.

The Zn-MOR structure with the lowest total energy contains the Al atom in the T1 position and the Zn^{2+} cation symmetrically accommodated in the 6MR (Figure 4a, top right). A detailed sketch of the most stable Zn-MOR structure is given in Figure 5. It shows that the Zn^{2+} cation interacts with four O atoms, two of them bonding to the Al atom. In this location the cation resides almost completely in the plane of the O-atoms allowing the effective four-coordination of the Zn^{2+} cation by the O-atoms of the framework. This configuration agrees well with the location of Zn^{2+} cations in the zeolite BEA. For this zeolite a combination of EXAFS and structure simulation indicates a preferential location of the cation in the 6MR, most likely those facing the main channel.[10] Note that the T1 site is among the less stable sites for the Al/Si substitution (Table 1). The good stabilization of this particular structure must therefore result from a good fit of the Zn^{2+} cation into the 6MR and from the symmetrical positions of both the Al atom and the Zn^{2+} cation within the 6MR. In the other two rings (6MR and 5MR) containing the T1 site the Zn^{2+} cation is much less stable. When located in the other 6MR with the Al atom situated in the corner

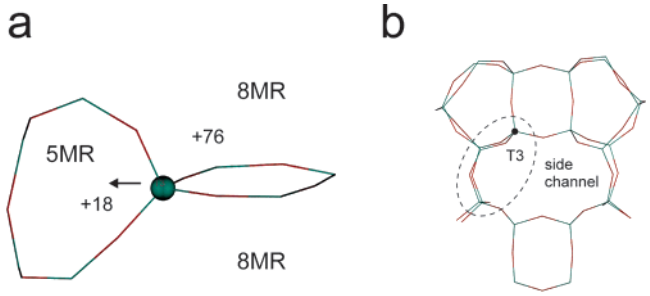

Figure 6. Relative stability of the Zn-MOR structures resulting from the Al/Si substitution in the T3 site in the zeolite side channel compensated with the extraframework Zn^{2+} cation. Energies (kJ/mol) are given relative to the most stable structure with Zn in the 6MR (cf. Figures 4 and 5).

(Figure 4a, right), the contact of the Zn^{2+} cation with the O atoms of the framework is less effective and such a Zn-MOR structure is disadvantaged by 41 kJ/mol compared with the most stable structure (Figure 5). A destabilization by 73 kJ/mol is observed for Al in the T1 site and the Zn^{2+} cation in the 5MR.

In contrast to the Al/Si substitution in the T1 site, for which the location of the Zn^{2+} cation in the 5MR is the least stable, for Al/Si substitutions in the T2 or T4 site the Zn^{2+} cation prefers a location in the 5MR. This means that the location of the isolated Al/Si substitutions in the T2 and T4 sites drives the extraframework Zn^{2+} cation into the 5MR. The most stable structure with Zn^{2+} in the 5MR is observed for Al in the T2 site. For this site the location of the cation in the 6MR is disadvantaged by a penalty of 69 kJ/mol. A destabilizing factor is the corner location of the Al atom and probably also a looser contact between the Zn^{2+} cation and the O atoms of the 6MR. The Zn-MOR structures with the Al atom in the T2 site and Zn^{2+} in the 8MR and in the 5MR exhibit similar stabilities, +25 and +21 kJ/mol, respectively. Slightly lower in energy, however, is the Zn^{2+} cation on the 5MR.

The Al/Si substitution in the T4 site of the framework is destabilized by ~7.5 kJ/mol (Table 1 and Figure 2). The Zn-MOR structures resulting from an isolated Al/Si substitution in the T4 site and compensated by a Zn^{2+} cation are considerably less stable than structures with the Al atom in the T1 and the T2 sites. Compared with the most stable structure (Al in T1, Zn in 6MR, cf. above) the two possible structures are by 91 (Zn in 8MR) and 76 kJ/mol (Zn in 5MR) higher in energy. Al/Si substitutions in the T4 sites of the framework thus clearly drive the extraframework Zn^{2+} cations into positions on the 5MR.

3.2.2. Zn^{2+} Located Close to an Isolated Al/Si Substitution in the Side Channel. Total energy differences of Zn-MOR structures resulting from an Al/Si substitution in the T3 site compensated by a Zn^{2+} cation are displayed in Figure 6. In the 8MR, connecting the side channel with the main channel, the Zn^{2+} cation is destabilized by 76 kJ/mol compared to the lowest-energy configuration (Al in T1, Zn in 6MR, cf. Figure 4). The most favorable location of the Zn^{2+} cation in the side channel of the mordenite structure is within the 5MR. Stabilization is achieved through four contacts with the O atoms of the narrow channel, three of them neighboring with the Al atom (not displayed). Note that this structure belongs to the most stable Zn-MOR structures. It is, however, hidden in the side channel and difficult to access from the zeolite main channel. For this reason the Zn-MOR structure based on a substitution in the T3 site is probably catalytically not active.

3.3. Stable Zn-MOR Structures. *3.3.1. Comparison of Stabilities.* In Figure 7 the relative energies of locally stable

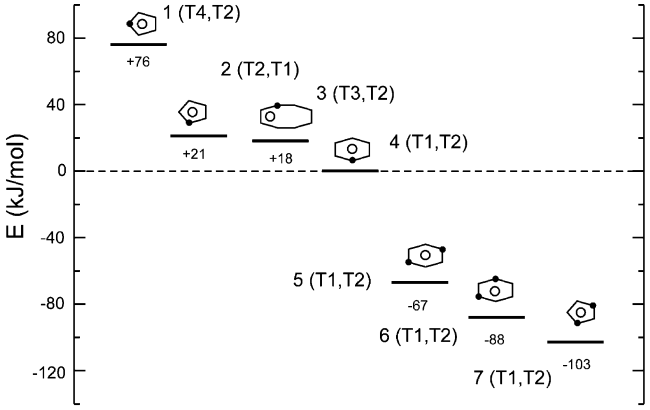

Figure 7. The most stable Zn-MOR structures for large Al−Al distances (structures **1**−**4**) and for short Al−Al distances (structures **5**−**7**). Symmetries of Al sites are given in parentheses. In structures **1**−**4** the Zn^{2+} cation is connected to the Al site indicated first. Full (empty) circles in the sketch of the zeolite structure show the location of the framework Al (extraframework Zn) atom.

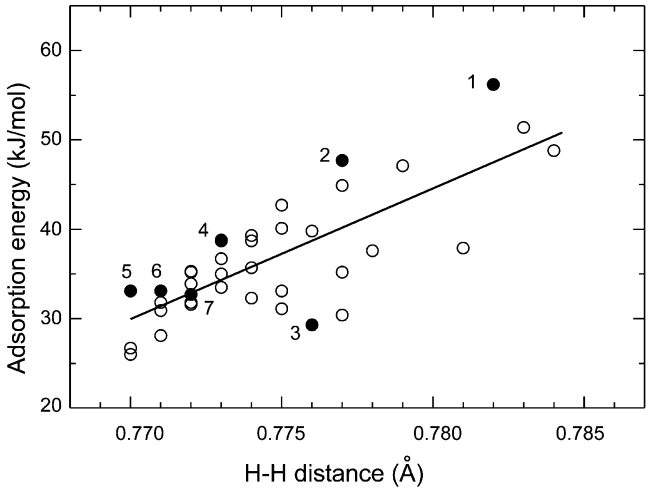

Figure 8. Correlation between the adsorption energy of H_2 on Zn^{2+} Lewis site in Zn-MOR and the H−H distance. The full line is a least-squares fit. Numbers indicate the structures displayed in Figure 7.

Zn-MOR structures with large Al−Al distances are compared with structures containing two Al/Si substitutions placed at short distances. The reference level is the energy of the most stable Zn-MOR structure with large Al−Al distance with Al in T1 and Zn in the 6MR (cf. Figure 4). The first four structures represent the locally stable configurations with Al atoms placed at a large distance and the Zn^{2+} cation connected to the Al/Si substitution in different T sites (T1−T4) (cf. Figures 4 and 6). Figure 7 demonstrates that small differences in energies of single Al/Si substitutions (cf. Table 1) lead to much larger differences in the total energies of Zn-exchanged structures. According to the total energies for the Zn-MOR structures optimized with respect to the location of the extraframework Zn^{2+} cation at fixed Al/Si substitutions we observe the following order (decreasing energy). The highest energy is found for the Al/Si substitution in the T4 site (structure 1) followed by structures with the Al atom in the T2, T3, and T1 site. In the first two structures the stable position of the Zn^{2+} cation is within the 5MR. The other two structures accommodate the extraframework cation in the side channel consisting of the 8MR and in the 6MR. The energy difference between the most stable and the least stable structures is 76 kJ/mol. Note that the only reason for this large energy difference in stabilities of Zn-MOR structures with large Al−Al distances is the location of Al in different tetrahedral sites of the mordenite structure.

The structures with two Al/Si substitutions in a small ring are energetically considerably more stable than those with large Al−Al distances. The much better stabilization is caused by the contact of Zn^{2+} with O atoms bonding to both Al/Si substitutions. As already shown above (Figure 2) the Al/Si substitutions located at short distances are disadvantaged only if they violate Loewensteins rule, i.e., if the Al sites share one O atom. Substitutions in the second-neighbor positions even lead to the most favorable configurations (Figure 2). This observation is confirmed for structures containing extraframework Zn^{2+} cations (Figure 7). Among structures **5** and **6** with the Zn^{2+} cation in the 6MR, structure **6** with two Al/Si substitutions in second-neighbor positions is lower in energy, because the Zn^{2+} cation makes more effective contact with both sites. The most stable configuration with two Al atoms exchanged in the tetrahedral sites and one extraframework Zn^{2+} cation is structure **7** with two Al/Si substitutions in the 5MR placed in second-neighbor positions (T1, T2), but excluding the less stable T4 site.

The analysis of the structural and NMR data indicates that in zeolites produced under laboratory conditions no Al−Si−Al sequence with Al atoms in the next-nearest-neighbor positions is observed.[43,44] On the basis of this observation the 2Al/5MR avoidance rule prohibiting the presence of two Al atoms in the same 5MR was introduced.[43] Processes of the zeolite manufacturing take advantage of structure directing agents (SDA) that help to build the zeolite framework. Functional groups of the SDA attract more ionic Al atoms and control their distribution in the zeolite framework. The use of different SDA results in different Al distributions.[44] Bulky molecules used as SDA, however, have a tendency to place Al atoms at large distances. For this reason in low-Al zeolites the formation of Al−Si−Al sequences is unlikely. Our calculations show that the formation of such sequences is not energetically forbidden and two Al atoms can occupy T sites in a small ring like 5MR and 6MR.

3.3.2. Adsorption of H_2. The adsorption strength of a large series of Zn^{2+} Lewis sites (we have examined altogether 35 different configurations shown in Figure 2a,b not violating the Loewensteins rule) sampled via the adsorption of H_2 is compared in Figure 8. The interaction of Zn^{2+} with the electron density of the H_2 molecule leads to a flat configuration with Zn−H distances of ∼1.95 Å. The transfer of electron density toward the cation makes the H−H bond weaker. In Figure 8 the adsorption energies of H_2 and the H−H bond length are compared for a set of Zn-MOR structures including all typical stable locations of the extraframework Zn^{2+} cation compared in Figure 7 above.

In the free molecule the calculated H−H distance is 0.750 Å. Upon adsorption on Zn^{2+} in Zn-MOR the H−H distance is elongated to values ranging between 0.77 and 0.785 Å (cf. Figure 8). The calculated adsorption energies range from 25 to 56 kJ/mol. Despite considerable scatter of the correlation a linear dependence is observed as evidenced by the least-squares fit. The values for the structures discussed in detail above and compared in Figure 7 are indicated by full circles. The adsorption strength of a Lewis site indirectly depends on the stability of the Zn-MOR configuration. Less stable structures adsorb a H_2 molecule more strongly and cause the largest activation of the H−H bond. On the other hand, adsorption energies for the most stable structures are lower and the adsorption leads only to a modest activation of the H−H bond. The energetic order displayed in Figure 7, however, is not

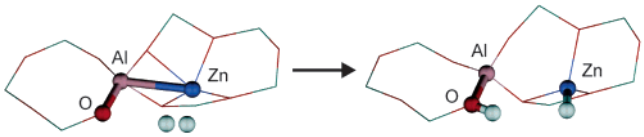

Figure 9. Reaction pathway for the dissociation of H_2 on Zn-MOR (configuration 1). The adsorbed neutral molecule (left) and the Brønsted acid site and the $[ZnH]^+$ cation produced by the dissociation (right).

completely valid for the activation of the H−H bond and for corresponding adsorption energies.

The three most stable structures (**5**, **6**, **7**) exhibit very similar adsorption energies. With lower stability (structures **4**, **2**, **1**) the adsorption energy increases proportionally. The exception is configuration **3** with the Zn atom in the side channel. The extremely low adsorption energy of this structure is due to the handicapped adsorption in a small void. The H−H distance observed for configuration **3**, however, reasonably fits the correlation between stabilities and activation of H_2. Note that the effect of the activation of the H−H bond is larger for configurations with Zn atoms in the 5MR's (**1**, **2**, **7**) than in 6MR's (**4**, **5**, **6**). In Figure 8 the most stable structure **7** exhibits even a larger activation effect than structures **5** and **6** and with Zn^{2+} in the 6MR. The stable structures (**5**, **6**, **7**) exhibit almost identical low adsorption energies. The activation of H_2, however, is inversely proportional to the total energies (Figure 7). In all these configurations two Al atoms are located in a small ring and increasing activation correlates with decreasing Al−Al distance. This phenomenon could mean that for an efficient activation of H_2 on Lewis sites of metal-exchanged zeolites a high concentration of Al in the framework might be important.

3.3.3. Reaction Pathways for the Dissociation of H_2 on Zn-MOR. The H_2 molecules adsorbed on Zn^{2+} are easily dissociated as demonstrated by experimental[11,12] and theoretical[20,21] studies. The dissociation

$$H_2 \rightarrow H^- + H^+ \qquad (1)$$

reduces the charge separation in Zn^{2+}-MOR^{2-} according to

$$MOR^{2-}\text{-}Zn^{2+} + H_2 \rightarrow H\text{-}MOR^{1-}\text{-}[Zn\text{-}H]^+ \qquad (2)$$

The dissociation products are proton and a hydride anion. The proton connects to the zeolite framework thus restoring a Brønsted acid site and the anion binds to the Zn^{2+} Lewis site forming a $[Zn\text{-}H]^+$ cation. Both products of the dissociation are detected by DRIFT spectra. In Zn-exchanged MFI (ZSM-5) the continuous formation of Brønsted acid sites leads to an increasing intensity of the O−H stretching band at 3610 cm^{-1} and the formation of the Zn−H^+ ion is detected by the growing intensity of the Zn−H stretching band at 1934 cm^{-1}.[12] Upon dissociation of H_2 the charge of the framework containing two Al/Si substitutions decreases from −2 to −1. The bonding of Zn^{2+} with the H^- anion produces a $[Zn\text{-}H]^+$ cation again reducing the ionic charge from +2 to +1. Figure 9 shows a sketch of the dissociation reaction.

The capacity of the Lewis sites 1 to 7 to dissociate the H_2 molecule is compared in Figure 10. For each Zn-MOR configuration the energy difference $\Delta E = E^{tot}_{diss} - E^{tot}_{ads}$ presents the total energy of the dissociated products relative to the adsorbed neutral molecule, i.e., the heat of the dissociation reaction. For a dissociation on the energetically most disadvantaged structure **1** dissociation is exothermic by 63 kJ/mol. For more stable Lewis sites the exothermicity diminishes smoothly to a value of 22 kJ/mol for the most stable configuration **7**. For Lewis sites 2 and 4, however, a much smaller ability to dissociate H_2 is observed compared to the trend outlined by the dotted line.

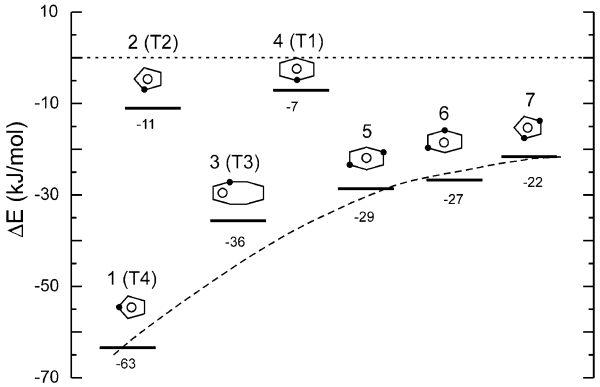

Figure 10. Dissociation energies of H_2 on Zn-MOR. For all configurations compared in Figure 7 $\Delta E = E^{tot}_{diss} - E^{tot}_{ads}$ is displayed. The negative values show that dissociative adsorption stabilizes all configurations irrespective of the position of the Zn^{2+} cation.

Upon dissociation of H_2 the H^- anion binds to the Zn^{2+} cation and the H^+ proton goes to a framework O site. Because of the location of Zn^{2+} in the extraframework position in the main channel the bonding of H^- to Zn^{2+} is energetically equivalent for all configurations. The capacity of a Lewis site in Zn-MOR to dissociate H_2 is thus driven by the ability of the framework to locally stabilize the proton. A stable accommodation of H^+ is possible on a O site bound to the framework Al site. Each Al site is surrounded by four O sites. Some of them, however, cannot accommodate the proton. The reason can be that such an O site is inaccessible from the main channel. The O sites in the ring on which the Zn^{2+} cation is deposited are not stabilizing, because they are in direct contact with the extraframework cation. A location of the proton on such an O site leads to a destabilizing repulsion between the positively charged $[ZnH]^+$ cation and H^+. Ideal for the accommodation of H^+ is an O site of another ring in the framework sharing the Al site with the ring on which the Zn^{2+} cation is deposited. A configuration with the high capacity to locally stabilize the proton represents a reaction pathway for the dissociation of H_2. The most exothermic reaction pathway is configuration **1** with initial and final states displayed in Figure 9. This has the highest energy among the Zn-MOR structures compared in Figure 7 because of the large separation of two Al atoms and because one of the Al atoms is located in the disadvantaged T4 site. The T4 site is a tetrahedral site connecting the 5MR and the 4MR. When an Al atom is located in the T4 site, the compensating Zn^{2+} cation resides in the 5MR (cf. Figure 4). The O site of the 4MR is located a short distance from the 5MR. This atom stays in contact with the molecule adsorbed on Zn (Figure 9, left) and is able to accommodate the proton released upon dissociation (Figure 9, right).

Configurations **5**, **6**, and **7** contain two Al atoms in one small ring. Because of the direct contact of two Al atoms with the compensating Zn^{2+} cation these structures exhibit a low energy but at the same time a decrease of reactivity. All these configurations, however, contain O sites with the capacity to accommodate a proton. Figure 10 shows that despite a reduced reactivity configurations **5**, **6**, and **7** represent exothermic reaction pathways for the dissociation of H_2.

In structure **2** the Al atom occupies the favorable T2 site in the 5MR and the Zn^{2+} cation is in contact with four O atoms of the same 5MR. Two O sites of the AlO_4 tetrahedron are part of the 5MR and are therefore unable to accommodate protons. One O site is oriented toward a dense part of the framework

and therefore not accessible from the main channel. The last O site is linked in Al−O−Si bonds extended along the main channel (along the *c* direction). These bonds exhibit rather limited flexibility. For an efficient stabilization of the proton, however, a high local flexibility of the structure is necessary.[49] Because none of the O atoms of the AlO_4 tetrahedron can accommodate the proton, configuration **2** does not represent a favorable reaction pathway for the dissociation of H_2. In contrast a high local deformability of the mordenite structure in the vicinity of the 5MR is observed for bonds oriented in the directions *a* and *b*, making the main channel more oval. This flexibility favors the reaction pathway of configuration **1**. The Zn-MOR configurations **3** and **4** have considerably lower energy than configurations **1** and **2** (cf. Figure 7). Both configurations do not support the dissociation of H_2. For configuration **4** the reason is again a limited flexibility of the Al−O−Si bonds extended along the *c* direction. Configuration **3** seemingly fits the dotted line outlined for reaction pathways in Figure 10. The negative value of the displayed energy difference $\Delta E = E_{diss}^{tot} - E_{ads}^{tot}$, however, is not due to the good stabilization of the proton, but originates in a low adsorption energy of H_2 (cf. Figure 8). Because the Zn^{2+} cation located in the side channel is a poor adsorption center the structure **3** does not represent a reaction pathway.

The energetics of the dissociative adsorption of H_2 on different Lewis sites shows that Zn-MOR structures are efficient catalysts for dissociation of H_2 irrespective of the position of the extraframework Zn^{2+} cation and the location of the Al/Si substitutions in the framework. The most exothermic, however, are energetically least favorable Lewis sites. Most efficient Zn-MOR configurations, i.e., those with high capacity to locally stabilize the proton, represent a reaction pathway for the dissociation of H_2.

3.3.4. Adsorption and Dissociation of CH₄. A first step in the conversion of hydrocarbons on active centers in zeolites is the breaking of a C−H bond. Zn-exchanged zeolites are efficient catalysts for hydrocarbon conversion. At temperatures as low as 475 K, conversion is seen for methane and ethane adsorbed in Zn-exchanged MFI (ZSM-5).[50,51] The proton released upon protolytic dissociation of alkanes binds framework oxygen atoms. The corresponding O−H stretching frequency is observed in DRIFT spectra at 3610 cm^{-1}.[50,51]

Total energies of CH_4 molecularly and dissociatively adsorbed on a series of Zn-MOR structures are listed in Table 2. The heat of reaction for dissociation $\Delta E = E_{diss}^{tot} - E_{ads}^{tot}$ for a series of Zn-MOR Lewis sites is compared in Figure 11. The variation of ΔE across the series of Lewis sites with increasing stability is similar to that for dissociation of H_2 (cf. Figure 10). The values of ΔE, however, are shifted upward by approximately 55 kJ/mol, except that configuration **1** dissociation of methane on a Zn^{2+} Lewis site is always endothermic. In the gas phase the dissociation energies $\Delta_r H°$ of H_2 and CH_4,

$$H^- + H^+ \rightarrow H_2 \qquad (3)$$

and

$$CH_3^- + H^+ \rightarrow CH_4 \qquad (4)$$

are 1675 and 1743.5 ± 2.9 kJ/mol, respectively.[52] The difference in the dissociation energies is 68.5 ± 2.9 kJ/mol, i.e., only slightly larger than the differences of 55 kJ/mol observed for the dissociation of the two molecules on Lewis sites in Zn-MOR. Only configuration **1** is strong enough for an exothermic

TABLE 2: Energetics of Dissociative and Molecular Adsorption of CH_4 in Zn-MOR[a]

Zn-MOR structure	$\Delta E = E_{diss}^{tot} - E_{ads}^{tot}$	$E_{ads}(CH_4)$
1	−4.3	78.2
2	+39.0	65.6
3	+26.6	20.9
4	+42.4	55.9
5	+23.8	45.1
6	+27.7	44.1
7	+35.7	44.2

[a] Dissociation energy ΔE and adsorption energy E_{ads} in kJ/mol.

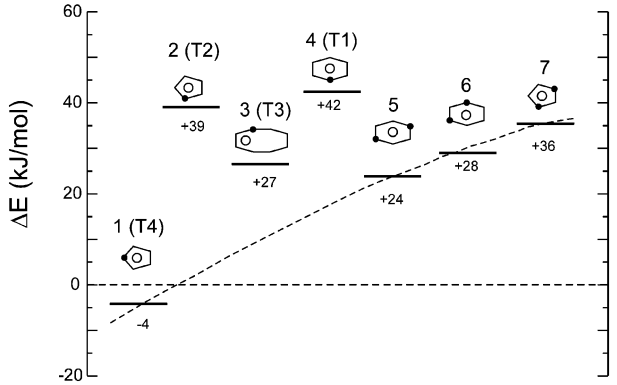

Figure 11. Dissociation energies for CH_4 on Zn^{2+} Lewis sites in Zn-MOR. The numbering of the different configurations is the same as in Figure 7.

C−H bond breaking in CH_4. The dissociation follows the alkyl path producing a carbanion and a proton[15,29] according to

$$MOR^{2-}\text{-}Zn^{2+} + CH_4 \rightarrow H\text{-}MOR^{1-}\text{-}[Zn\text{-}CH_3]^+ \qquad (5)$$

The methyl anion connects to the Zn^{2+} cation decreasing the charge from +2 to +1 and the proton goes to the most stabilizing O site of the framework.

No major difference is observed for the breaking C−H bond in CH_4 compared with the dissociation of the H−H bond (cf. Figure 10). The methyl anion connected to Zn^{2+} is placed approximately in the center of the channel. The variation of ΔE displayed in Figure 11 is driven by the ability of the different configurations to accommodate the proton. The same four configurations **1**, **5**, **6**, and **7** represent reaction pathways for the dissociation of H_2 and CH_4 (cf. Figures 10 and 11). The dissociation on the Lewis sites **2** and **4** is strongly disadvantaged because a low deformability of the Al−O−Si bonds extending along the main channel offers only a weak stabilization of the proton on the corresponding O atoms of the framework. For configuration **3** the dissociation energy is close to the dotted line outlined for reaction pathways only because of the extremely low adsorption energy of CH_4 on Zn^{2+} in the side channel. The adsorption energies of CH_4 on the Zn-MOR structures are given in Table 2. The largest value is 78.2 kJ/mol calculated for the adsorption on structure **1**. With decreasing adsorption strength of Zn-MOR the adsorption energy smoothly decreases to ∼44 kJ/mol. The only exception is structure **3** with the adsorption energy ∼21 kJ/mol, 3-times smaller than averaged adsorption energy of neighboring structures **2** and **4**. The calculated small adsorption energy of CH_4 on Zn^{2+} in the side channel is in agreement with experimental observations indicating preferable adsorption of molecules in the large channel of the zeolite structure. Because of disabled adsorption in the side channel structure **3** does not constitute a reaction pathway for the dissociation of adsorbed molecules.

3.4. Conclusions. Total energy DFT calculations of Al/Si substitutions on the T sites of mordenite distinguish between the more favorable T2 and T3 sites and the less favorable T1 and T4 sites. Most disadvantaged is a substitution on the T4 site with a penalty of 7.5 kJ/mol compared with the T2 site. For a large number of different combinations of two Al/Si substitutions the most favorable position of the Zn^{2+} cation is localized. Interestingly, for an Al atom in the T2 or the T4 site the most stable location of Zn^{2+} is on the 5MR.

The analysis of the distribution of Al atoms in the mordenite structure without a compensating cation shows that the total energy of the configuration hardly depends on the Al−Al distance. A penalty of 20−40 kJ/mol, found for nearest-neighbor Al−Al positions, is in agreement with the experimental Loewenstein rule. Slightly larger stabilization than the average value is observed for two Al atoms in the second-neighbor position, allowing a location of two Al atoms in a small ring, such as the 6MR and the 5MR.

The comparison of the total energies of configurations containing two Al atoms and one extraframework Zn^{2+} cation shows that the stability depends mainly on the location of the Al/Si substitution and on the Al−Al distance. Configurations with Al atoms placed at large distances lead to higher energy per the Zn^{2+} Lewis site. The energy penalty increases if Al atoms are placed in the disfavored T4 site. In the most favorable structure the Zn atom resides on the 5MR with good contact to two Al sites placed in the same 5MR. The energies of locally stable Zn-MOR configurations span an interval of ∼180 kJ/mol.

The activity and reactivity of Lewis sites in Zn-MOR is tested via the adsorption and dissociation of H_2 and CH_4. Because the dissociation produces protons, only those configurations represent efficient reaction pathways which favor the formation of a Brønsted site by binding a proton to a framework O site. The most efficient reaction pathway appears to be the energetically least favorable Lewis site with Al atoms placed at a large distance, containing the Al/Si substitution in the T4 site, and the Zn^{2+} cation in the 5MR. Configurations with Zn^{2+} located in the 6MR and in the side channel cannot accommodate protons in a stable position and therefore are not active centers for H_2 dissociation and C−H bond breaking.

The ability to split the H−H and the C−H bonds of adsorbed H_2 and CH_4 molecules is evaluated as a difference between the energies for molecular and dissociative adsorption (ΔE). The reactivity of a series of Lewis sites in Zn-MOR decreases with increasing stability. For H_2 dissociation ΔE varies between −63 kJ/mol for the most reactive configuration and −22 k/mol for the less reactive and more stable structures. Hence even for the most stable Lewis site in Zn-MOR dissociation of H_2 is by 22 kJ/mol more favorable than adsorption of a neutral H_2 molecule. For CH_4 the variation of ΔE exhibits a similar shape. It is, however, shifted upward by ∼55 kJ/mol. This value calculated for the dissociation on the Zn^{2+} cations in MOR agrees well with the difference in enthalpies of the acid dissociation in the gas phase of 68.5 ± 2.9 kJ/mol. Because of this shift only the most reactive Lewis sites in Zn-MOR can break C−H bonds.

The analysis of a variety of Lewis sites in Zn-MOR shows that stronger reaction centers are expected to be formed in low-Al zeolites with Al atoms placed at large distances. The Zn-activated structures of such zeolites, however, are less stable. At higher concentrations of Al atoms substituted on T sites of the framework considerably more stable structures can be formed containing two Al atoms in one small ring, like the 6MR and the 5MR. Such stable structures support the dissociation of H_2, but are unable to catalyze the breaking of C−H bonds in hydrocarbons. The Al/Si substitution in the T4 site of mordenite always leads to the formation of sites with increased reactivity. The success of the fabrication of strong Lewis sites in mordenite and in zeolites in general therefore requires targeted substitution of Al atoms into the specific T site of the zeolite framework.

Acknowledgment. This work has been supported by the Austrian Science Funds under project No. P17020-PHYS and by the Institut Français du Pétrole. Computational resources were partly granted by the Computing Center of Vienna University (Schrödinger cluster).

References and Notes

(1) Mole, T.; Anderson, J. R. *Appl. Catal.* **1985**, *17*, 127.
(2) Ono, Y. *Rev. Sci. Eng.* **1992**, *34*, 179.
(3) Hagen, A.; Roessner, F. *Catal. Rev.* **2000**, *42*, 403.
(4) Iglesia, E.; Baumgartner, E. *Catal. Today* **1996**, *31*, 207.
(5) Müller, T. E. In *Encyclopedia of Catalysis*; Horvath, I. T., Ed.; Wiley: New York, 2002.
(6) Onyestak, G. Y.; Papp, J.; Kallo, D. In *Studies in Surface Science and Catalysis*; Karge, H. G., Weitkamp, J., Eds.; Elsevier: Amsterdam, The Netherlands, 1989; Vol. 46, p 241.
(7) Biscardi, J. A.; Meitzner, G. D.; Iglesia, E. *J. Catal.* **1998**, *179*, 192.
(8) Biscardi, J. A.; Iglesia, E. *Catal. Today* **1996**, *31*, 207.
(9) Elmalki, El-M.; van Santen, R. A.; Sachtler, W. M. H. *J. Phys. Chem. B* **1999**, *103*, 4611.
(10) Penzien, J.; Abraham, A.; van Bokhoven, J. A.; Jentys, A.; Muller, T. E.; Sievers, C.; Lercher, J. A. *J. Phys. Chem. B* **2004**, *108*, 4116.
(11) Kazansky, V. B.; Borovkov, V. Y.; Serikh, A. I.; van Santen, R. A.; Anderson, G. D. *Catal. Lett.* **2000**, *66*, 39.
(12) Kazansky, V. B. *J. Catal.* **2003**, *216*, 192.
(13) Kazansky, V. B.; Serykh, A. I. *Phys. Chem. Chem. Phys.* **2004**, *6*, 3760.
(14) Barbosa, L. A. M. M.; van Santen, R. A. *Catal. Lett.* **1999**, *63*, 97.
(15) Frash, M. V.; van Santen, R. A. *Phys. Chem. Chem. Phys.* **2000**, *2*, 1085.
(16) Barbosa, L. A. M. M.; Zhidomirov, G. M.; van Santen, R. A. *Phys. Chem. Chem. Phys.* **2000**, *2*, 3909.
(17) Rice, M. J.; Chakraborty, A. K.; Bell, A. T. *J. Phys. Chem. B* **2000**, *104*, 9987.
(18) Barbosa, L. A. M. M.; van Santen, R. A. *J. Mol. Catal. A* **2001**, *166*, 101.
(19) Barbosa, L. A. M. M.; Zhidomirov, G. M.; van Santen, R. A. *Catal. Lett.* **2001**, *77*, 55.
(20) Shubin, A. A.; Zhidomirov, G. M.; Yakovlev, A. L.; van Santen, R. A. *J. Phys. Chem. B* **2001**, *105*, 4928.
(21) Shubin, A. A.; Zhidomirov, G. M.; Kazansky, V. B.; van Santen, R. A. *Catal. Lett.* **2003**, *90*, 137.
(22) Zhidomirov, G. M.; Shubin, A. A.; Kazansky, V. B.; van Santen, R. A. *Int. J. Quantum Chem.* **2004**, *100*, 489.
(23) McMillan, S. A.; Snurr, R. A.; Broadbelt, L. J. *Microporous Mesoporous Mater.* **2004**, *68*, 45.
(24) Rice, M. J.; Chakraborty, A. K.; Bell, A. T. *J. Catal.* **2000**, *194*, 278.
(25) Barbosa, L. A. M. M.; van Santen, R. A.; Hafner, J. *J. Am. Chem. Soc.* **2001**, *123*, 4530.
(26) Barbosa, L. A. M. M.; van Santen, R. A. *J. Phys. Chem. B* **2003**, *107*, 14342.
(27) Barbosa, L. A. M. M.; van Santen, R. A. *J. Phys. Chem. B* **2003**, *107*, 4532.
(28) Kachurovskaya, N. A.; Zhidomirov, G. M.; van Santen, R. A. *Res. Chem. Intermed.* **2004**, *30*, 99.
(29) Benco, L.; Bucko, T.; Hafner, J.; Toulhoat, H. In *Studies in Surface Science and Catalysis*; Cejka, J., Zilkova, N., Nachtigall, P., Eds.; Elsevier: Amsterdam, 2005; Vol. 158, p 939.
(30) Demuth, T.; Hafner, J.; Benco, L.; Toulhoat, H. *J. Phys. Chem. B* **2000**, *104*, 4593.
(31) Benco, L.; Bucko, T.; Hafner, J.; Toulhoat, H. *J. Phys. Chem. B* **2004**, *108*, 13656.
(32) Kresse, G.; Hafner, J. *J. Phys. Chem. B* **1993**, *48*, 13115.
(33) Kresse, G.; Hafner, J. *J. Phys. Chem. B* **1994**, *49*, 14251.
(34) Kresse, G.; Furthmüller, J. *Comput. Mater. Sci.* **1996**, *6*, 15.
(35) Kresse, G.; Furthmüller, J. *Phys. Rev. B* **1996**, *54*, 11169.
(36) Perdew, J. P.; Zunger, A. *Phys. Rev. B* **1981**, *23*, 5048.
(37) Perdew, J. P.; Chevary, A.; Vosko, S. H.; Jackson, K. A.; Pedersen, M. R.; Singh, D. J.; Fiolhais, C. *Phys. Rev. B* **1992**, *46*, 6671.
(38) Vanderbilt, D. *Phys. Rev. B* **1990**, *41*, 7892.
(39) Kresse, G.; Hafner, J. *J. Phys. Condens. Matter* **1994**, *6*, 8245.

(40) Blöchl, P. E. *Phys. Rev. B* **1994**, *50*, 17953.
(41) Kresse, G.; Joubert, D. *Phys. Rev. B* **1999**, *59*, 1758.
(42) Jeanvoine, Y.; Angyan, J.; Kresse, G.; Hafner, J. *J. Phys. Chem. B* **1998**, *102*, 5573.
(43) Takaishi, T.; Kato, M.; Itabashi, K. *Zeolites* **1995**, *15*, 21.
(44) Kato, M.; Itabashi, K.; Matsumoto, A.; Tsutsumi, K. *J. Phys. Chem. B* **2003**, *107*, 1788.
(45) Shiokawa, S.; Ito, M.; Itabashi, K. *Zeolites* **1989**, *9*, 170.
(46) Löwenstein, W. *Am. Miner.* **1954**, *39*, 92.
(47) Kazansky, V. B.; Serykh, A. I.; Bell, A. T. *Catal. Lett.* **2002**, *83*, 191.
(48) Kazansky, V. B.; Serykh, A. I.; Anderson, B. G.; van Santen, R. A. *Catal. Lett.* **2003**, *88*, 211.
(49) Benco, L.; Demuth, T.; Hafner, J.; Hutschka, F. *J. Chem. Phys.* **1999**, *111*, 7537.
(50) Kazansky, V. B.; Serykh, A. I.; Pidko, E. A. *J. Catal.* **2004**, *225*, 369.
(51) Kazansky, V. B.; Pidko, E. A. *J. Phys. Chem. B* **2004**, *109*, 2103.
(52) www.NIST.com.